

Homocysteine promotes scavenger receptor CD36 mediated oxLDL uptake eliciting PON2 antioxidant defense response in ARPE-19 and THP-1 macrophage cells

Kannadasan Anand Babu

R.S. Mehta Jain Department of Biochemistry and Cell Biology, KBIRVO, Vision Research Foundation, Sankara Nethralaya, Chennai; Dr. APJ Abdul Kalam Centre of Excellence in Innovation and Entrepreneurship, Dr. M.G.R. Educational and Research Institute, Chennai, India <https://orcid.org/0000-0002-9910-2044>

Parveen Sen

Shri Bhagwan Mahavir Vitreoretinal Services, Sankara Nethralaya, Chennai, India

Jyotirmay Biswas

Uveitis and Ocular Pathology Department, Sankara Nethralaya, Chennai, India

Narayanasamy Angayarkanni (drak@snmail.org)

R.S. Mehta Jain Department of Biochemistry and Cell Biology, KBIRVO, Vision Research Foundation, Sankara Nethralaya, Chennai, India <https://orcid.org/0000-0002-8147-1589>

Research Article

Keywords: Homocysteine, oxLDL, ARPE-19, Macrophage, CD36, Paraoxonase

Posted Date: May 12th, 2022

DOI: <https://doi.org/10.21203/rs.3.rs-1647955/v1>

License: This work is licensed under a Creative Commons Attribution 4.0 International License. [Read Full License](#)

Abstract

Oxidative stress is the major cause of dysfunctional phagocytic cells such as the macrophages causing atherosclerotic changes in cardiovascular disease (CVD) and the retinal pigment epithelium (RPE) showing lipofuscin accumulation seen in age-related macular degeneration (AMD). Systemic homocysteine (Hcy) is associated with CVD and AMD pathology. The study evaluated the prooxidant Hcy on the metabolic activity of ARPE-19 cells and THP-1 macrophage cells *in vitro*, since localized macrophages are involved in AMD pathology. These cells were exposed to Hcy and homocysteine thiolactone (HCTL) showed increased oxLDL uptake assessed by fluorimetry along with increased protein expression of oxLDL receptor, CD36 in both the cells. Cellular Paraonase 2 (PON2), an antioxidant was significantly increased in both ARPE-19 and THP-1 macrophages possibly to counteract the intracellular oxidative stress. The increased PON2 and CD36 expression observed were mediated by the increased SP1 and PPAR γ transcription factors, respectively. The lysosomal activity assessed in terms of cathepsin D expression was significantly increased indicating accumulation of the intracellular oxLDL. Further, immunohistochemistry revealed relatively higher expression of PON2 and CD36 in the RPE of AMD donor eye sections compared to control, supporting dysregulated oxLDL metabolism and antioxidant defense by PON2 enzyme observed *in vitro*. Thus, Hcy increases oxLDL uptake and promotes oxidative stress that potentially causes RPE dysfunction contributing to AMD pathology, while the cellular PON2 is promoted as an antioxidant response.

Introduction

Oxidized LDL can trigger inflammation through the activation of macrophages and other cells and has been associated with atherosclerotic plaque formation in cardiovascular disease [1]. Recently, we had shown that oxLDL promote cytokine release, macrophage infiltration and pro-angiogenic effect in ARPE-19 cells [2].

Several prooxidant metabolites are associated with LDL oxidation. Notably, Homocysteine (Hcy) can bring about LDL oxidation through modification in apolipoprotein B (apoB) of LDL [3].

Hyperhomocysteinemia and elevated levels of oxLDL could be the independent risk factor for cardiovascular diseases [4].

Hcy is a known pro-oxidant present also in vitreous [5] apart from systemic circulation [6]. Excess of Hcy may affect the RPE structure and function that progress to the development of AMD-like features [7]. Paraonase 2 (PON2) is an intracellular antioxidant enzyme induced by ROS [8] that can prevent the formation of oxLDL [9]. Elevated levels of plasma Hcy as well as homocysteine thiolactone (HCTL), are metabolites associated with the AMD pathology reported earlier [10–12]. Both oxLDL and Hcy promote reactive oxygen species (ROS) generation that is reduced with N-acetyl cysteine (NAC) treatment [2].

Earlier, we reported on the increased serum oxidized low-density lipoprotein (oxLDL) levels in AMD cases [13]. CD36 is the principal receptor for oxLDL uptake in macrophages involved in the atherosclerosis development [14], which is also expressed in RPE [15]. RPE dysfunction leads to the pathogenesis of AMD. Oxidative stress and deranged lipid metabolism in the RPE play a major role in the chronic inflammatory response in RPE that contributes to AMD pathogenesis [16–18].

Macrophage dysfunction is key in the pathogenesis of AMD [19]. Both RPE and macrophages are phagocytic cells that are involved in the process of engulfing the oxidized photoreceptor outer segments (POS) and apoptotic cells respectively [20]. The oxidized lipids from the POS is internalized by RPE through CD36 receptor [21] and over a period it leads to the accumulation of lipofuscin causing RPE degeneration [22]. Picard et al reported on the sub-RPE accumulation of oxLDL along with basement membrane thickening associated with AMD pathology [23]. However, there are limited studies on the role of oxLDL in AMD pathology.

This study explored how excess Hcy promotes AMD pathology at the level of RPE and tissue macrophages. The effect of the prooxidant on the oxLDL uptake in ARPE-19 cells as well as THP-1 macrophage cells were evaluated *in vitro*.

Materials And Methods

ARPE-19 culture:

Adult human Retinal Pigment Epithelial cells, ARPE-19 (ATCC-CRL-2302) was cultured with Dulbecco's Modified essential medium and F12 (DMEM/F12) (Sigma-Aldrich, USA) supplemented with 10% Fetal Bovine Serum (FBS) (Gibco, USA), Antibiotic-Antimycotic solution (Gibco, USA) for 3 weeks. After that, they were subjected to serum starvation for overnight and exposure was given in DMEM/F-12, supplemented with 1% FBS at various time point. Cells were used between passages 5 and 10.

THP-1 Macrophage culture:

Human monocytic cell line, THP-1 (Riken, Japan) was differentiated into macrophages by 50 ng/ml phorbol 12-myristate-13-acetate (PMA) for 48 hours under Roswell Park Memorial Institute 1640 (RPMI 1640) medium (Gibco, USA), supplemented with 10% FBS. After 48 hours, they were subjected to serum starvation for overnight and exposure was given in RPMI 1640, supplemented with 1% FBS at various time point.

LDL isolation by density gradient method:

Low-density Lipoprotein (LDL) was isolated from human plasma by density gradient method using Optiprep (60% Iodixanol solution) (Axis-Shield, Norway) by the method of Davies *et al* [24].

Dil Labelling of LDL, *in vitro* oxidation and validation:

The LDL was labelled with the fluorescent probe 1,1'-dioctadecyl-3,3',3'-tetramethyl-indocarbocyanine perchlorate (DiI) (Molecular Probes, USA) as per the standard protocol [25]. LDL was incubated with DiI (DiI-LDL) at 37°C for 16 h. Oxidized LDL (oxLDL) and DiI labelled oxLDL (DiI-oxLDL) were generated by incubating the plasma LDL and DiI-LDL with 10 μ M CuCl $_2$ at 37°C for 24 h respectively [26]. The oxidation of LDL was validated by various methods mentioned earlier [2]. The LDL preparations were stored at 4°C until use and used within a week of preparation or discarded.

DiI-oxLDL uptake assay by spectrofluorimetry:

Dil-oxLDL uptake was assessed by incubating Dil-oxLDL with cells cultured in 12 well plate for 2 hours at 37°C with various concentrations [27]. Specificity of uptake was determined with 5 to 10-fold excess of unlabelled oxLDL along with Dil-oxLDL. Dil-oxLDL uptake assay was performed after exposed to prooxidants for 3 h, ARPE-19 and THP-1 macrophage cells was incubated with 20 µg/mL and 50 µg/mL Dil-oxLDL for 2 h respectively, and the Dil-oxLDL uptake was measured in the cell lysate by fluorimetry. After incubation, cells were washed twice with 0.4% bovine serum albumin (BSA) in 1X PBS and washed thrice with 1X PBS and incubated the cells with 500 µl of lysis buffer (0.1% SDS, 0.1 M NaOH) for 30 min at room temperature (RT). Fluorescence was measured from the cell lysate on black microtiter plate in Spectramax (Molecular Devices, CA, USA) with excitation and emission set at 520 and 580 nm respectively. Cellular protein was determined by the Bradford method. Dil-oxLDL uptake was normalised to cellular protein [28].

Dil-oxLDL uptake study by fluorescent microscopy

The cells were seeded onto round coverslip in 24 well cell culture plate. Dil-oxLDL uptake assay was performed for 2 h in ARPE-19 and THP-1 macrophage cells with Dil-oxLDL (10 µg/mL) after exposed to prooxidants for 3 h. After Dil-oxLDL incubation, the cells were washed with 1X PBS for three times with shaking. Then the cells were fixed with 4% paraformaldehyde for 20 min at RT. After that, the cells were washed with 1X PBS for three times. The cell nuclei were stained with Hoechst stain (Sigma-Aldrich, USA) for five min and mounted using anti-fade mounting medium (Life Technologies, USA). The cells were observed under Axio Observer Z.1 microscope (Carl Zeiss, Germany). Intensity of the fluorescence was assessed using Image-J software (NIH, Bethesda, USA).

Gene expressions by Real-Time PCR:

The RNA was isolated from the experimentally treated cells by TRI reagent (Favorgen Biotech Corp, Taiwan) and the cDNA conversion was performed by iScript cDNA synthesis kit (Bio-Rad, USA). The cDNA was used to determine the gene expressions of *PON2*, *CD36*, *SP1* and *PPARγ* by Real-Time Polymerase Chain Reaction (qPCR), which was performed with the CFX96 Touch Real-Time detection system (Bio-Rad, USA) by SYBR Green chemistry (Bio-Rad, USA). The qPCR conditions were 95°C for 10 min, followed by 40 cycles of 95°C for 15 s, 60°C for 15 s and 72°C for 20 s. The comparative $2^{-\Delta\Delta Ct}$ method was used to analyse the results of the genes of interest relative to internal control gene (*18S rRNA*) [29]. The primer sequences were given in the Supplementary File 1 (Table S1).

Protein expression by western blot:

The cell lysate was prepared with lysis buffer and the total protein estimation was measured using Pierce BCA protein assay kit (ThermoFisher Scientific, USA) as per the manufacturer's instructions. The protein resolved in 10% SDS-PAGE was transferred onto Hybond-P PVDF membrane (Amersham Pharmacia Biotech, UK), blocked with 5% BSA and probed with 1: 2000 dilutions of primary antibodies for Cathepsin D (Cell Signaling Technology, USA), PON2, and CD36 (Santa Cruz Biotechnology, USA). Then the blot was probed with 1:20000 dilutions of corresponding HRP-conjugated secondary antibodies (Santa Cruz Biotechnology, Santa Cruz, CA, USA) and developed with Clarity™ Western ECL Substrate (Bio-Rad, USA) and the image was captured using FlourChem FC3 gel documentation system (Protein Simple, California, USA). β-actin was used as loading control. The loading control protein (β-actin) was reprobed with the same blot after performing the stripping protocol by immersing the blot with stripping buffer (62.5 mM Tris HCl, pH 6.8, 2% SDS, 0.8% β-mercaptoethanol) for 15 min at RT and then washed thoroughly with PBST twice for 10 min to ensure no traces of β-mercaptoethanol left on the membrane; finally two more washes with 1X PBS. The intensity of the bands was assessed using ImageJ software (NIH, Bethesda, USA) and normalized to β-actin.

Culturing of senescent ARPE-19 cells:

The ARPE-19 cells was converted to prematurely senescent cells by repetitive oxidative stress as previously described [30]. Confluent ARPE-19 cells grown in T25 cell culture flasks were treated daily with 6mM *tert*-Butyl hydroperoxide (tBHP) for 1 h at 37°C. After stress, the cells were washed twice with 1X PBS and allowed to recover in complete culture medium for 24 h. The procedure of tBHP treatment was repeated for 5 consecutive days. After the last tBHP treatment, the cells were allowed to recover for 3 days before we conducted further experiments. The cells were then trypsinized and replated at various densities, depending on the experiments.

Analysis of senescence-associated β-galactosidase activity in ARPE-19:

The senescent cells shown to have β-galactosidase activity, which was detectable at pH 6.0, termed as senescent-associated β-galactosidase activity (SA-βgal). This activity was distinct from the acidic β-galactosidase activity (lysosomal) detectable at pH 4.0, present in all cells. The SA-βgal activity was determined by using the chromogenic substrate 5-bromo-4-chloro-3-indolyl β-D-galactopyranoside (X-gal), which yields an insoluble blue compound when cleaved by β-galactosidase in senescent cells at pH 6.0. The SA-βgal activity was strongly associated with senescent cells alone, since it was not detectable in quiescent cells or terminally differentiated cells [31]. After exposure, the culture medium was removed and washed the cells with 1X PBS twice. The senescent ARPE-19 cells (sARPE-19) were fixed with X-gal fix buffer (5 mM EGTA, 2 mM MgCl₂, 0.2% glutaraldehyde in 0.1 M phosphate buffer, pH 7.3) for 15 min at RT. After fixation, the cells were washed with X-gal wash buffer (2 mM MgCl₂ in 0.1 M phosphate buffer, pH 7.3) twice for 5 min each. Then the cells were incubated with X-gal staining buffer (2 mM MgCl₂, 5 mM potassium ferrocyanide, 5 mM potassium ferricyanide, 1 mg/mL X-gal in 0.1 M phosphate buffer, pH 7.3) in 37°C for 12–16 h. After staining, the cells were washed with 1X PBS twice and took images under bright field through Nikon Eclipse Ts2 microscope (Nikon Instruments Inc., USA) at 20X magnification.

Immunofluorescence based detection of PON2 and CD36 in RPE of AMD and Control donor eye tissues:

The donor eyeballs were obtained from the CU Shah Eye Bank, Medical Research foundation, Chennai. Deparaffinization of wax-embedded tissue sections were done using stored blocks of AMD and Control Donor eye using xylene for 10 min (twice) and hydrated with 100% ethanol for 4 min (twice), followed by 95%, 80%, 70%, and 60%, ethanol treatment for 4 min each. Finally, the tissue sections were rinsed with distilled water. Tissue sections were used for Haematoxylin and Eosin (H & E) staining and observed under bright field microscope to assess the histology characteristic of control and AMD. The remaining sections were used for the immunofluorescence studies. Antigen retrieval was performed by incubating the tissue sections with 0.05% Trypsin solution at 37°C for 30 min. The tissue sections were washed with 1X PBS twice and blocked with 1% BSA in PBS for 30 min at RT. Subsequently, the tissue sections were incubated with primary PON2 and CD36 antibodies at 4°C for overnight in a moisture chamber to avoid evaporation. The tissue sections were washed with 1X PBST (1X PBS with 0.1% Tween-20) twice and incubated with fluorescein isothiocyanate (FITC)-conjugated secondary antibody (Life Technologies, USA) for 1 h 30 min in the dark at RT, counterstained with Hoechst stain and mounted using 50% glycerol in PBS. The tissue sections were observed under fluorescence microscope (Life Technologies, USA). AMD eye was identified by the pathologist based on the drusens and degenerative RPE compared to the control eye in the H & E-stained sections of the donor eyes.

Statistical analysis:

All data were expressed as Mean \pm SEM of three independent experiments done not less than triplicate unless indicated. Statistical significance was assessed by Student's t-test. $p < 0.05$ was considered as statistically significant.

Results

Homocysteine as prooxidant promotes oxLDL uptake in ARPE-19 and THP-1 Macrophages:

In order to find if Hcy influences lipofuscin formation through oxLDL uptake by RPE and by tissue macrophages, labelled oxLDL uptake was studied in the presence of Hcy in ARPE-19 cells and in THP-1 macrophage cells *in vitro*.

As DiI-oxLDL uptake measured by spectrofluorimetry showed a dose-dependent increase in ARPE-19 and THP-1 macrophages. Specificity of uptake was determined with a 5 to 10-fold excess of unlabelled oxLDL, which shows a fall in the labelled uptake, compared to DiI labelled alone (Fig. S1a and S1b). There was a time-dependent increase in DiI-oxLDL uptake observed in ARPE-19 and THP-1 macrophages (Fig. S1c and S1d).

The oxLDL uptake was significantly increased on treatment with Hcy, HCTL ($p < 0.05$), hydrogen peroxide (H_2O_2) ($p < 0.01$) in both ARPE-19 and THP-1 macrophage cells. The NAC treatment significantly reduced the DiI-oxLDL uptake induced by H_2O_2 condition in both ARPE-19 ($p < 0.05$) and THP-1 macrophages ($p < 0.001$) (Fig. 1a and 1b).

In addition, immunofluorescence images also revealed that oxLDL uptake was significantly increased in the cells exposed to the prooxidant conditions in both ARPE-19 and THP-1 macrophage cells ($p < 0.05$). The NAC treatment significantly reduced the DiI-oxLDL uptake induced by H_2O_2 condition in both ARPE-19 and THP-1 macrophages ($p < 0.05$) (Fig. 2). This confirms that increased oxLDL uptake is promoted by the prooxidants such as Hcy in the cells studied.

Homocysteine promotes scavenger receptor expression in ARPE-19 and THP-1 macrophages:

Scavenger receptor CD36 is responsible for the oxLDL uptake in both RPE and macrophage cells. Since oxLDL uptake was increased under prooxidant conditions, CD36 protein expression was studied in ARPE-19 and THP-1 macrophage cells under prooxidant conditions. CD36 protein expression was significantly increased under all the prooxidant conditions at all the time point in ARPE-19 cells (Fig. 3a). A significant increase in oxLDL uptake was observed within 3 hours, and the overall CD36 protein expression was increased under prooxidants conditions at all the time points in THP-1 macrophage cells (Fig. 3b). 3 hour seems to be suitable for the macrophage.

Regulation of CD36 expression by PPAR γ under prooxidant insults:

The transcription factor, peroxisome proliferator-activated receptor gamma (PPAR γ) is involved in modulating the *CD36* gene expression. Hence, the *CD36* and *PPAR γ* gene expression was studied under prooxidants conditions in ARPE-19 and THP-1 macrophage cells. *PPAR γ* gene expression was found to be increased at 3 h exposure and showed a decreased trend over time in ARPE-19 cells (Fig. 4a). However, *PPAR γ* gene expression was increased with exposure time in THP-1 macrophage cells unlike an early response in 3 h as seen in ARPE-19 cells (Fig. 4b).

Homocysteine promotes PON2 expression in ARPE-19 and THP-1 macrophages:

As oxLDL uptake is increased under the oxidative stress conditions, PON2 protein expression was studied as it prevents oxidation and promotes LDL regeneration. PON2 protein expression was significantly increased under all prooxidants at all the time points. NAC pre-treatment to H_2O_2 treated cells at 24 hours in both ARPE-19 and THP-1 macrophage cells did not improve PON expression but was significantly reduced compared to H_2O_2 alone treated cells indicating ROS induced PON2 expression (Fig. 5).

Regulation of PON2 expression by SP1 under prooxidant insults:

SP1 is one of the key transcription factors regulating PON2 expression in ARPE-19 cells as reported in our earlier study in ARPE-19 under oxidative stress condition. Hence, *SP1* gene expression was studied under these prooxidant conditions in ARPE-19 and THP-1 macrophage cells. *SP1* gene expression was significantly increased under the prooxidant conditions in ARPE-19 cells and THP-1 macrophage cells. SP1 gene expression was significantly increased with oxLDL treatment at all the time points studied and increased expression was seen with Hcy and HCTL treatment as well (Fig. 6).

Effect of prooxidants on Cathepsin D expression in ARPE-19 and THP-1 macrophages:

As oxLDL uptake increased in ARPE-19 and THP-1 macrophages under prooxidants conditions, the lysosomal activity of ARPE-19 and THP-1 macrophage cells under prooxidant conditions were studied in terms of cathepsin D protein expression by western blot. The cathepsin D protein expression was found to be higher at 3 h and 24 h exposure in ARPE-19 cells on exposure to the prooxidant metabolites. At 72 h exposure, cathepsin D protein expression was increased under oxLDL exposure but decreased under Hcy, HCTL and H_2O_2 exposure (Fig. 7a). In THP-1 macrophages, there was initial drop in cathepsin D expression at 3 h exposure which was increased at 24 h and 72 h (Fig. 7b).

Role of PON2 and scavenger receptor in oxLDL uptake in senescent ARPE-19:

In order to relate more closely to the RPE in AMD pathology, the ARPE-19 cells were subjected to senescence by tBHP treatment. Senescence was proven by SA- β gal activity (Fig. 8a). Like ARPE-19, the DiI-oxLDL uptake was significantly increased under oxidative stress conditions in sARPE-19 (Fig. 8b). The PON2 protein expression in sARPE-19 was significantly increased with prooxidant treatments. NAC treatment did not abrogate the H_2O_2 induced PON2 similar to the 72 h treatment in normal ARPE-19 cells as shown in Fig. 5. The CD36 protein expression was significantly increased under the oxidative stress conditions, and it was further increased under NAC treatment. The cathepsin D protein expression was significantly reduced under the oxidative stress conditions, and it was reversed by the NAC treatment (Fig. 8c).

PON2 and CD36 expression in RPE of AMD and Control eye tissues:

To further infer, we analysed the PON2 and CD36 expression in RPE of AMD and control donor eye tissues which is devoid of AMD related changes such as absence of drusen and RPE alterations. The PON2 and CD36 expression were found to be higher in the RPE of AMD eye tissues compared to control (Fig. 9).

Discussion

Evidence from various studies suggests that RPE cells are prone to oxidative stress [32]. The oxLDL is a trigger for early events in the pathogenesis of AMD, since the metabolism of oxLDL and ROS generation can promote RPE dysfunction and augmented apoptosis [33]. Serum LDL and oxLDL readily enters the retina through the choriocapillaries via RPE [34]. ApoB, a major protein in the LDL and oxLDL molecules are reportedly present in the cholesterol-containing drusen and the basal deposits in human eyes with AMD [35]. Hcy mediated accumulation of cholesterol in THP-1 macrophages has been shown [36, 37]. However, the accumulation of oxLDL mediated by Hcy warrants more studies. Macrophages and RPE interactions are reported to be associated with AMD pathology [38, 39]. Though, plasma Hcy association with AMD pathology is reported [40–42] the cellular pathology triggered by Hcy at the level of RPE is incompletely understood.

This study therefore focussed on the localized effects of these systemic prooxidants namely Hcy and oxLDL associated with AMD pathology that were evaluated in both ARPE-19 as well as in THP-1 macrophage cells *in vitro*. An augmented oxLDL uptake by ARPE-19 cells and THP-1 macrophages were observed in cells exposed to Hcy and its thiolactone form along with increased expression of CD36 and PPAR γ in both the cells. The CD36 receptor is the principal receptor, responsible for oxLDL uptake and plays an important role in the clearance of oxLDL in ARPE-19 cells [23]. The CD36 transcription and oxLDL uptake could be induced by the activation of PPAR γ [43]. Thus, this study reveals that Hcy induces oxLDL uptake that promotes cellular stress. The cellular response in ARPE-19 cells due to Hcy and oxLDL promoting inflammation and chemotaxis of macrophage cells was earlier reported by us [2]. Malfunction of choroidal macrophages and RPE leads to incomplete removal of debris from sub-RPE and transported to the choroid that results in the development of drusen and basal lamina deposits [19]. Further, there is oxidative stress response in RPE with the increased phagocytic and metabolic activity [44].

PON, an antioxidant enzyme (PON1 and PON3) prevents oxidation of LDL at systemic level [45]. Elevated protein levels and PON activity is reported by us in AMD [13] and at cellular level (PON2) [9]. As the oxidative stress potentially increases in response to Hcy and HCTL mediated accumulation of oxLDL, the antioxidant PON2 protein expression was evaluated in ARPE-19 and THP-1 macrophages that showed an increased expression, mediated by increased SP1 transcription factor. This is suggestive of a defense mechanism that seems to set in to metabolise the oxLDL and counteract the intracellular oxidative stress. We earlier reported on such a defense in chlorpyrifos induced oxidative stress in ARPE-19 cells *in vitro*, wherein such an increase in PON enzyme activities and PON2 expression was observed mediated by SP1 transcription factor [8]. There are other similar reports as well [9, 46].

As there is increased oxLDL uptake, accumulation of oxidized cholesterol esters in lysosomes can occur [47, 48]. Hence, the lysosomal activity in terms of cathepsin D expression in ARPE-19 and THP-1 macrophages was studied. In ARPE-19 cells, the cathepsin D protein expression was significantly increased under oxidative stress. The oxLDL promoted the cathepsin D expression in ARPE-19 cells. The oxidized lipids generated by the prooxidants are known to induce RPE and macrophage degeneration under chronic conditions due to lysosomal destabilization [49], apart from inflammation and apoptosis were reported [2]. In THP-1 macrophage cells, there was initial drop in cathepsin D expression at short exposure (3 h) but the expression increased with time *in vitro* (24 and 72 h). Previous reports suggest that uptake of oxLDL in macrophage results in partial lysosomal enzyme inactivation and relocation to the cytosol contributing to poor degradation activity of lysosomes [50, 51].

We further evaluated the key observations in the cultured premature senescent ARPE-19 cells (sARPE-19) to relate closely to AMD pathology. The oxLDL uptake in sARPE-19 was found to be increased under oxidative stress conditions similar to the observation in ARPE-19 cells. The antioxidant response was significant in terms of PON2 protein expression in sARPE-19 under oxidative stress conditions similar to the observations in ARPE-19 cells. However, unlike ARPE-19, NAC treatment in sARPE-19 did not alter the oxLDL uptake that was increased by H₂O₂ treatment. Higher concentration of NAC needs to be evaluated. A significant increase in CD36 protein expression under the oxidative stress conditions was similar to that of ARPE-19. However, NAC treatment seems to further augment the CD36 expression in sARPE-19 unlike ARPE-19 that showed no such increase. A significant decrease in the cathepsin D protein expression in sARPE-19 was seen similar to ARPE-19 cells (72 h) revealing that the lysosomal activity is drastically reduced under prolonged oxidative stress which improves with the NAC treatment. NAC thus improved the CD36 and cathepsin D expression in the senescence model of ARPE-19 cells exposed to prooxidant metabolites associated with AMD pathology.

Further, PON2 and CD36 expression were found to be increased in RPE of AMD eye tissues compared to control tissues based on immunolocalization, which supports the inference from the *in vitro* data. There are no reports up to our knowledge that have studied about the PON2 and CD36 expression in RPE of AMD eye tissues. Increased PON2 expression localized to RPE is observed in this study in the AMD eyes for the first time and therefore, PON2 might be considered as disease marker of oxidative stress in AMD, apart from being a systemic marker as reported by us earlier [13]. Prolonged increase in CD36 expression also observed in the AMD eyes results in oxLDL accumulation causes oxidative stress in the RPE cells apart from direct ROS generation by Hcy as reported in the *in vitro* studies in ARPE-19 [2]. Antioxidant response in terms of PON expression is observed, while treatment with antioxidants can be beneficial in improving the cathepsin D activity and therefore in the rescue of lysosomal activity. Autophagy and proteasomal clearance are thus promoted by the lysosomal activity of hydrolases including cathepsin D in AMD [52, 53]. Though increased cathepsin D immunoreactivity around drusen was reported the enzyme activity is crucial [54]. Loss of cathepsin D activity initiated by oxidative stress contributes to accumulation of undegraded substrates, inflammasome formation leading to RPE dysfunction apoptosis and AMD pathogenesis [55].

Conclusion

The metabolites Hcy and HCTL as prooxidants induced the oxLDL uptake in both ARPE-19 similar to THP-1 macrophages. The oxLDL uptake was mediated through scavenger receptor CD36. The antioxidant PON2 expression was increased to counteract the intracellular oxidative stress in ARPE-19 and THP-1 macrophages. CD36 and PON2 expressions were increased in AMD eyes. The lysosomal activity in terms of cathepsin D expression was triggered in ARPE-19 cells which seems to decrease with time unlike THP-1 macrophage cells which was prominent in the early phase. Similarly, the susceptibility of RPE to oxLDL accumulation was also observed in senescent ARPE-19 that showed increased CD36 expression but decreased cathepsin D activity indicating RPE dysfunction, promoting AMD pathogenesis. Thus, this study supports senescent models of ARPE-19 to explore AMD pathogenesis. While PON2 increase is proposedly a biomarker of AMD pathology, interventions to promote lysosomal activity such as the antioxidants can be beneficial.

Abbreviations

AMD, Age-related Macular Degeneration; apoB, Apolipoprotein B; BSA, Bovine Serum Albumin; Dil, 1,1'-dioctadecyl-3,3',3'-tetramethyl-indocarbocyanine perchlorate; FBS, Fetal Bovine Serum; FITC, Fluorescein isothiocyanate; H & E, Haematoxylin and Eosin; HCTL, Homocysteine thiolactone; Hcy, Homocysteine; LDL, Low-Density Lipoprotein; NAC, N-acetyl cysteine; oxLDL, oxidized LDL; PBS, Phosphate-Buffered Saline; oxBST, Phosphate-Buffered Saline with 0.1% Tween-20; PMA, Phorbol 12-myristate-13-acetate; PON, Paraoxonase; POS, Photoreceptor Outer Segment; qPCR, Real-Time Polymerase Chain Reaction; ROS, Reactive Oxygen Species; RPE, Retinal Pigment Epithelium; RT, Room Temperature; SA- β gal, senescent-associated β -galactosidase; SEM, Standard error of the mean; tBHP, tert-Butyl Hydroperoxide; X-gal, 5-bromo-4-chloro-3-indolyl β -D-galactopyranoside.

Declarations

Funding: This work was supported by the DBT, Govt. of India (Grant Number: BT/PR13630/BRB/10/776/2010) and ICMR, Govt. of India (Grant Number: BMS/FW/BIOCHEM/2015-21610/JUN-2015/15/TN/PVT).

Conflicts of interest/Competing interests: Not applicable

Availability of Data and Material: The data that support the findings of this study are available as additional supporting files.

Code availability: Not applicable

Ethical approval: Not applicable

Consent to participate: Not applicable

Consent for publication: Not applicable

Author's contributions:

Anand Babu K: Writing - original draft preparation, Methodology, Formal analysis and investigation.

Parveen Sen: Clinical validation.

Jyotirmay Biswas: Clinical Investigation.

Narayanamy Angayarkanni: Supervision, Conceptualisation, Validation, Writing – Review and Editing.

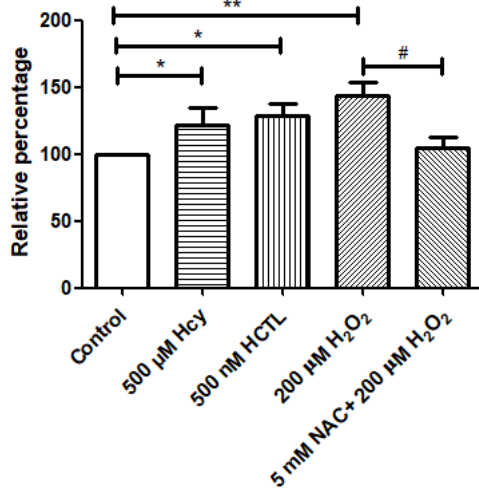
References

1. Poznyak AV, Nikiforov NG, Markin AM, et al (2021) Overview of OxLDL and Its Impact on Cardiovascular Health: Focus on Atherosclerosis. *Frontiers in Pharmacology* 11:
2. AnandBabu K, Sen P, Angayarkanni N (2019) Oxidized LDL, homocysteine, homocysteine thiolactone and advanced glycation end products act as pro-oxidant metabolites inducing cytokine release, macrophage infiltration and pro-angiogenic effect in ARPE-19 cells. *PLoS ONE* 14:e0216899. <https://doi.org/10.1371/journal.pone.0216899>
3. Vidal M, Sainte-Marie J, Philippot J, Bienvenue A (1986) Thiolation of low-density lipoproteins and their interaction with L2C leukemic lymphocytes. *Biochimie* 68:723–30
4. Kumar Singh N, Suri A, Kumari M, Kaushik P (2022) A study on serum homocysteine and oxidized LDL as markers of cardiovascular risk in patients with overt hypothyroidism. *Horm Mol Biol Clin Investig*. <https://doi.org/10.1515/hmbci-2021-0029>
5. Coral K, Angayarkanni N, Gomathy N, et al (2009) Homocysteine levels in the vitreous of proliferative diabetic retinopathy and rhegmatogenous retinal detachment: its modulating role on lysyl oxidase. *Investigative ophthalmology & visual science* 50:3607–12. <https://doi.org/10.1167/iovs.08-2667>
6. Devi SRB, Suganeswari G, Sharma T, et al (2012) Homocysteine induces oxidative stress in young adult central retinal vein occlusion. *The British journal of ophthalmology* 96:1122–6. <https://doi.org/10.1136/bjophthalmol-2011-301370>
7. Ibrahim AS, Mander S, Hussein KA, et al (2016) Hyperhomocysteinemia disrupts retinal pigment epithelial structure and function with features of age-related macular degeneration. *Oncotarget* 7:8532–45. <https://doi.org/10.18632/oncotarget.7384>
8. Jasna JM, Anandbabu K, Bharathi SR, Angayarkanni N (2014) Paraoxonase enzyme protects retinal pigment epithelium from chlorpyrifos insult. *PLoS one* 9:e0101380. <https://doi.org/10.1371/journal.pone.0101380>
9. Ng CJ, Wadleigh DJ, Gangopadhyay A, et al (2001) Paraoxonase-2 Is a Ubiquitously Expressed Protein with Antioxidant Properties and Is Capable of Preventing Cell-mediated Oxidative Modification of Low Density Lipoprotein. *Journal of Biological Chemistry* 276:44444–44449. <https://doi.org/10.1074/jbc.M105660200>
10. <https://doi.org/10.4103/0971-5916.192026>
11. Coral K, Raman R, Rathi S, et al (2006) Plasma homocysteine and total thiol content in patients with exudative age-related macular degeneration. *Eye (London, England)* 20:203–207. <https://doi.org/10.1038/sj.eye.6701853>
12. Huang P, Wang F, Sah BK, et al (2015) Homocysteine and the risk of age-related macular degeneration: a systematic review and meta-analysis. *Scientific reports* 5:10585. <https://doi.org/10.1038/srep10585>
13. AnandBabu K, Bharathidevi S, Sripriya S, et al (2016) Serum Paraoxonase activity in relation to lipid profile in Age-related Macular Degeneration patients. *Experimental eye research* 152:100–112. <https://doi.org/10.1016/j.exer.2016.09.009>
14. BOULLIER A, BIRD DA, CHANG M-K, et al (2006) Scavenger Receptors, Oxidized LDL, and Atherosclerosis. *Annals of the New York Academy of Sciences* 947:214–223. <https://doi.org/10.1111/j.1749-6632.2001.tb03943.x>
15. Hayes KC, Lindsey S, Stephan ZF, Brecker D (1989) Retinal pigment epithelium possesses both LDL and scavenger receptor activity. *Investigative ophthalmology & visual science* 30:225–232
16. Jarrett S, Boulton M (2012) Consequences of oxidative stress in age-related macular degeneration. *Molecular Aspects of Medicine* 33:399–417. <https://doi.org/10.1016/j.mam.2012.03.009>. CONSEQUENCES
17. Xu Q, Cao S, Rajapakse S, Matsubara JA (2018) Understanding AMD by analogy: Systematic review of lipid-related common pathogenic mechanisms in AMD, AD, AS and GN. *Lipids in Health and Disease* 17:1–13. <https://doi.org/10.1186/s12944-017-0647-7>
18. Zarbin M a (2004) Current Concepts in the Pathogenesis of Age-Related Macular Degeneration. *Cell* 122:598–614
19. Chen M, Chan C-C, Xu H (2018) Cholesterol homeostasis, macrophage malfunction and age-related macular degeneration. *Annals of Translational Medicine* 6:S55. <https://doi.org/10.21037/21877>
20. Finnemann SC, Rodriguez-Boulton E (1999) Macrophage and Retinal Pigment Epithelium Phagocytosis: Apoptotic Cells and Photoreceptors Compete for α v β 3 and α v β 5 Integrins, and Protein Kinase C Regulates α v β 5 Binding and Cytoskeletal Linkage. *The Journal of experimental medicine* 190:861–874

21. Sun M, Finnemann SC, Febbraio M, et al (2006) Light-induced oxidation of photoreceptor outer segment phospholipids generates ligands for CD36-mediated phagocytosis by retinal pigment epithelium: A potential mechanism for modulating outer segment phagocytosis under oxidant stress conditions. *Journal of Biological Chemistry* 281:4222–4230. <https://doi.org/10.1074/jbc.M509769200>
22. Parmar VM, Parmar T, Arai E, et al (2018) A2E-associated cell death and inflammation in retinal pigmented epithelial cells from human induced pluripotent stem cells. *Stem Cell Research* 27:95–104. <https://doi.org/10.1016/j.scr.2018.01.014>
23. Picard E, Houssier M, Bujold K, et al (2010) CD36 plays an important role in the clearance of oxLDL and associated age-dependent sub-retinal deposits. *Aging* 2:981–9
24. Davies IG, Graham JM, Griffin BA (2003) Rapid separation of LDL subclasses by iodixanol gradient ultracentrifugation. *Clinical chemistry* 49:1865–72
25. Dehock B, Fenart L, Dehouck MP, et al (1997) A new function for the LDL receptor: transcytosis of LDL across the blood-brain barrier. *The Journal of cell biology* 138:877–89
26. Jenkins AJ, Velarde V, Klein RL, et al (2000) Native and modified LDL activate extracellular signal-regulated kinases in mesangial cells. *Diabetes* 49:2160–9
27. Stephan ZF, Yurachek EC (1993) Rapid fluorometric assay of LDL receptor activity by DiI-labeled LDL. *Journal of lipid research* 34:325–30
28. Teupser D, Thiery J, Walli AK, Seidel D (1996) Determination of LDL- and scavenger-receptor activity in adherent and non-adherent cultured cells with a new single-step fluorometric assay. *Biochimica et biophysica acta* 1303:193–8
29. Schmittgen TD, Livak KJ (2008) Analyzing real-time PCR data by the comparative CT method. *Nature Protocols* 3:1101–1108. <https://doi.org/10.1038/nprot.2008.73>
30. Liao WL, Turko I V. (2009) Accumulation of large protein fragments in prematurely senescent ARPE-19 cells. *Investigative Ophthalmology and Visual Science* 50:4992–4997. <https://doi.org/10.1167/iovs.09-3671>
31. Dimri GP, Lee X, Basile G, et al (1995) A biomarker that identifies senescent human cells in culture and in aging skin in vivo. *Proceedings of the National Academy of Sciences of the United States of America* 92:9363–9367. <https://doi.org/10.1073/pnas.92.20.9363>
32. Liang FQ, Godley BF (2003) Oxidative stress-induced mitochondrial DNA damage in human retinal pigment epithelial cells: A possible mechanism for RPE aging and age-related macular degeneration. *Experimental Eye Research* 76:397–403. [https://doi.org/10.1016/S0014-4835\(03\)00023-X](https://doi.org/10.1016/S0014-4835(03)00023-X)
33. Yamada Y, Tian J, Yang Y, et al (2008) Oxidized low density lipoproteins induce a pathologic response by retinal pigmented epithelial cells. *Journal of neurochemistry* 105:1187–97. <https://doi.org/10.1111/j.1471-4159.2008.05211.x>
34. Gordiyenko N, Campos M, Lee JW, et al (2004) RPE cells internalize low-density lipoprotein (LDL) and oxidized LDL (oxLDL) in large quantities in vitro and in vivo. *Investigative ophthalmology & visual science* 45:2822–9. <https://doi.org/10.1167/iovs.04-0074>
35. Malek G, Li C-M, Guidry C, et al (2003) Apolipoprotein B in cholesterol-containing drusen and basal deposits of human eyes with age-related maculopathy. *The American journal of pathology* 162:413–25. [https://doi.org/10.1016/S0002-9440\(10\)63836-9](https://doi.org/10.1016/S0002-9440(10)63836-9)
36. Ide N, Keller C, Weiss N (2006) Aged Garlic Extract Inhibits Homocysteine-Induced CD36 Expression and Foam Cell Formation in Human Macrophages. *The Journal of Nutrition* 136:755S-758S. <https://doi.org/10.1093/jn/136.3.755S>
37. Liang Y, Yang X, Ma L, et al (2013) Homocysteine-mediated cholesterol efflux via ABCA1 and ACAT1 DNA methylation in THP-1 monocyte-derived foam cells. *Acta Biochimica et Biophysica Sinica* 45:220–228. <https://doi.org/10.1093/abbs/gms119>
38. Otsuki Y, Ito E, Mukai A, et al (2021) CD63 + extracellular vesicles from retinal pigment epithelial cells participate in crosstalk with macrophages in the innate inflammatory axis. *Experimental Eye Research* 205:108496. <https://doi.org/10.1016/j.exer.2021.108496>
39. Yamawaki T, Ito E, Mukai A, et al (2016) The ingenious interactions between macrophages and functionally plastic retinal pigment epithelium cells. *Investigative Ophthalmology and Visual Science* 57:5945–5953. <https://doi.org/10.1167/iovs.16-20604>
40. Coral K, Raman R, Rathi S, et al (2006) Plasma homocysteine and total thiol content in patients with exudative age-related macular degeneration. *Eye (London, England)* 20:203–207. <https://doi.org/10.1038/sj.eye.6701853>
41. Ibrahim AS, Mander S, Hussein KA, et al (2016) Hyperhomocysteinemia disrupts retinal pigment epithelial structure and function with features of age-related macular degeneration. *Oncotarget* 7:8532–45. <https://doi.org/10.18632/oncotarget.7384>
42. Pinna A, Zaccheddu F, Boscia F, et al (2018) Homocysteine and risk of age-related macular degeneration: a systematic review and meta-analysis. *Acta Ophthalmologica* 96:e269–e276. <https://doi.org/10.1111/aos.13343>
43. Yu M, Jiang M, Chen Y, et al (2016) Inhibition of Macrophage CD36 Expression and Cellular Oxidized Low Density Lipoprotein (oxLDL) Accumulation by Tamoxifen: A PEROXISOME PROLIFERATOR-ACTIVATED RECEPTOR (PPAR) γ -DEPENDENT MECHANISM. *The Journal of biological chemistry* 291:16977–89. <https://doi.org/10.1074/jbc.M116.740092>
44. Datta S, Cano M, Ebrahimi K, et al (2017) The impact of oxidative stress and inflammation on RPE degeneration in non-neovascular AMD. *Progress in Retinal and Eye Research* 60:201–218. <https://doi.org/10.1016/j.preteyres.2017.03.002>
45. Rosenblat M, Aviram M (2009) Paraoxonases role in the prevention of cardiovascular diseases. *BioFactors (Oxford, England)* 35:98–104. <https://doi.org/10.1002/biof.16>
46. Chistiakov DA, Melnichenko AA, Orekhov AN, Bobryshev Y V. (2017) Paraoxonase and atherosclerosis-related cardiovascular diseases. *Biochimie* 132:19–27. <https://doi.org/10.1016/j.biochi.2016.10.010>
47. Dhaliwal BS, Steinbrecher UP (2000) Cholesterol delivered to macrophages by oxidized low density lipoprotein is sequestered in lysosomes and fails to efflux normally. *Journal of lipid research* 41:1658–65
48. Brown AJ, Mander EL, Gelissen IC, et al (2000) Cholesterol and oxysterol metabolism and subcellular distribution in macrophage foam cells. Accumulation of oxidized esters in lysosomes. *Journal of lipid research* 41:226–37
49. LI W, YUAN X-M (2004) Increased Expression and Translocation of Lysosomal Cathepsins Contribute to Macrophage Apoptosis in Atherogenesis. *Annals of the New York Academy of Sciences* 1030:427–433. <https://doi.org/10.1196/annals.1329.053>
50. Li W, Yuan XM, Olsson a. G, Brunk UT (1998) Uptake of Oxidized LDL by Macrophages Results in Partial Lysosomal Enzyme Inactivation and Relocation. *Arteriosclerosis, Thrombosis, and Vascular Biology* 18:177–184. <https://doi.org/10.1161/01.ATV.18.2.177>
51. Hoppe G, Neil JO, Hoff HF (1994) Inactivation of Lysosomal Proteases by Oxidized Low Density Lipoprotein Is Partially Responsible for Its Poor Degradation by Mouse Peritoneal Macrophages. *Journal of Clinical Investigation* 94:1506–1512
52. Bosch E, Horwitz J, Bok D (1993) Phagocytosis of outer segments by retinal pigment epithelium: phagosome-lysosome interaction. *Journal of Histochemistry & Cytochemistry* 41:253–263. <https://doi.org/10.1177/41.2.8419462>
53. RAKOCZY PE, LAI CM, BAINES M, et al (1997) Modulation of cathepsin D activity in retinal pigment epithelial cells. *Biochemical Journal* 324:935–940. <https://doi.org/10.1042/bj3240935>
54. RAKOCZY PE, Sarks SH, Daw N, CONSTABLE IJ (1999) Distribution of Cathepsin D in Human Eyes with or without Age-related Maculopathy. *Experimental eye research* 69:367–374
55. Kaarniranta K, Sinha D, Blasiak J, et al (2013) Autophagy and heterophagy dysregulation leads to retinal pigment epithelium dysfunction and development of age-related macular degeneration. *Autophagy* 9:973–84. <https://doi.org/10.4161/auto.24546>

Figures

a. Dil-oxLDL uptake assay in ARPE-19



b. Dil-oxLDL uptake assay in THP-1 Macrophage

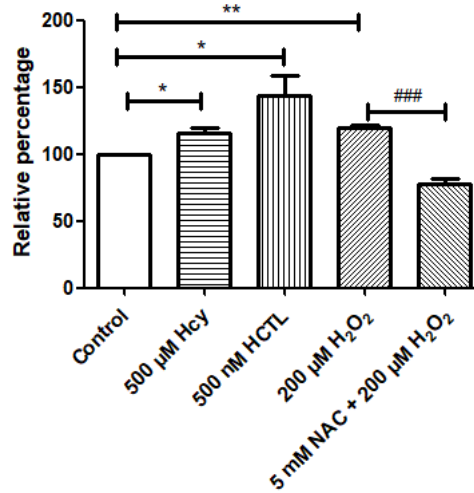
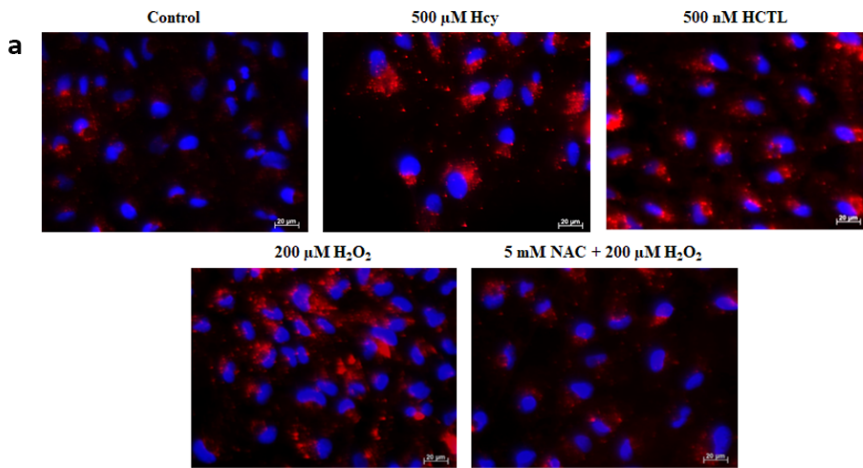


Figure 1

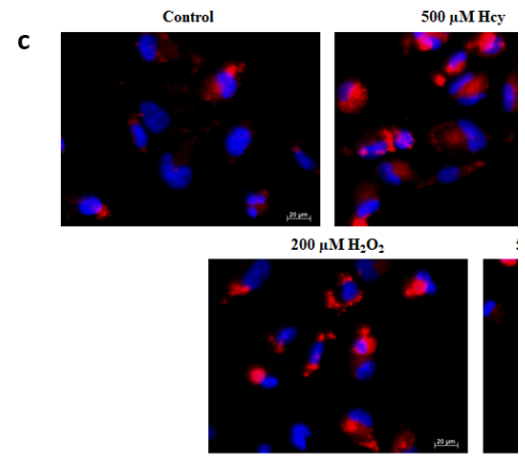
Dil-oxLDL uptake assay in ARPE-19 and THP-1 macrophages by spectrofluorimetry

Dil-oxLDL uptake assay in ARPE-19 and THP-1 macrophages was performed with Dil labelled oxLDL. Dil-oxLDL uptake was measured in cell lysate of (a) ARPE-19 and (b) THP-1 macrophage cells exposed to Hcy, HCTL, H₂O₂ and NAC + H₂O₂ conditions for 3 h by fluorimetry. H₂O₂, a known prooxidant and NAC, a known antioxidant were used as the controls. The bar graph represented as relative percentage to control. The data are expressed as Mean ± SEM of three independent experiments done not less than triplicate. *#p < 0.05, **p < 0.01, ###p < 0.001, considered as significant. *Control vs prooxidants, #H₂O₂ vs NAC + H₂O₂.

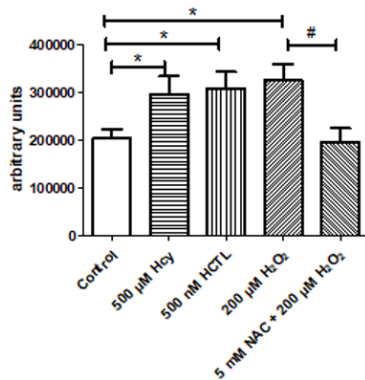
ARPE-19



THP-1 Macro



b. Dil-oxLDL uptake assay in ARPE-19



d. Dil-oxLDL uptake assay in

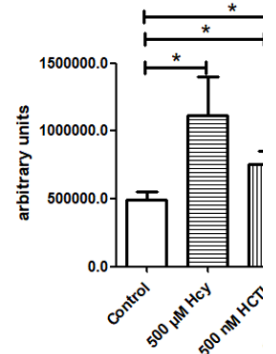


Figure 2

Dil-oxLDL uptake assay in ARPE-19 and THP-1 macrophage by immunofluorescence

Dil-oxLDL uptake was measured in (a) ARPE-19 and (b) THP-1 macrophage cells exposed to Hcy, HCTL, H₂O₂ and NAC + H₂O₂ conditions based on the pink immunofluorescence of the Dil. The bar graph showing the pixel intensity of the fluorescence analysed in (c) ARPE-19 and (d) THP-1 macrophages images by Image J software. The values are expressed as Mean ± SEM of three independent experiments done not less than triplicate. *#*p* < 0.05, considered as significant. *Control vs prooxidants, #H₂O₂ vs NAC + H₂O₂.

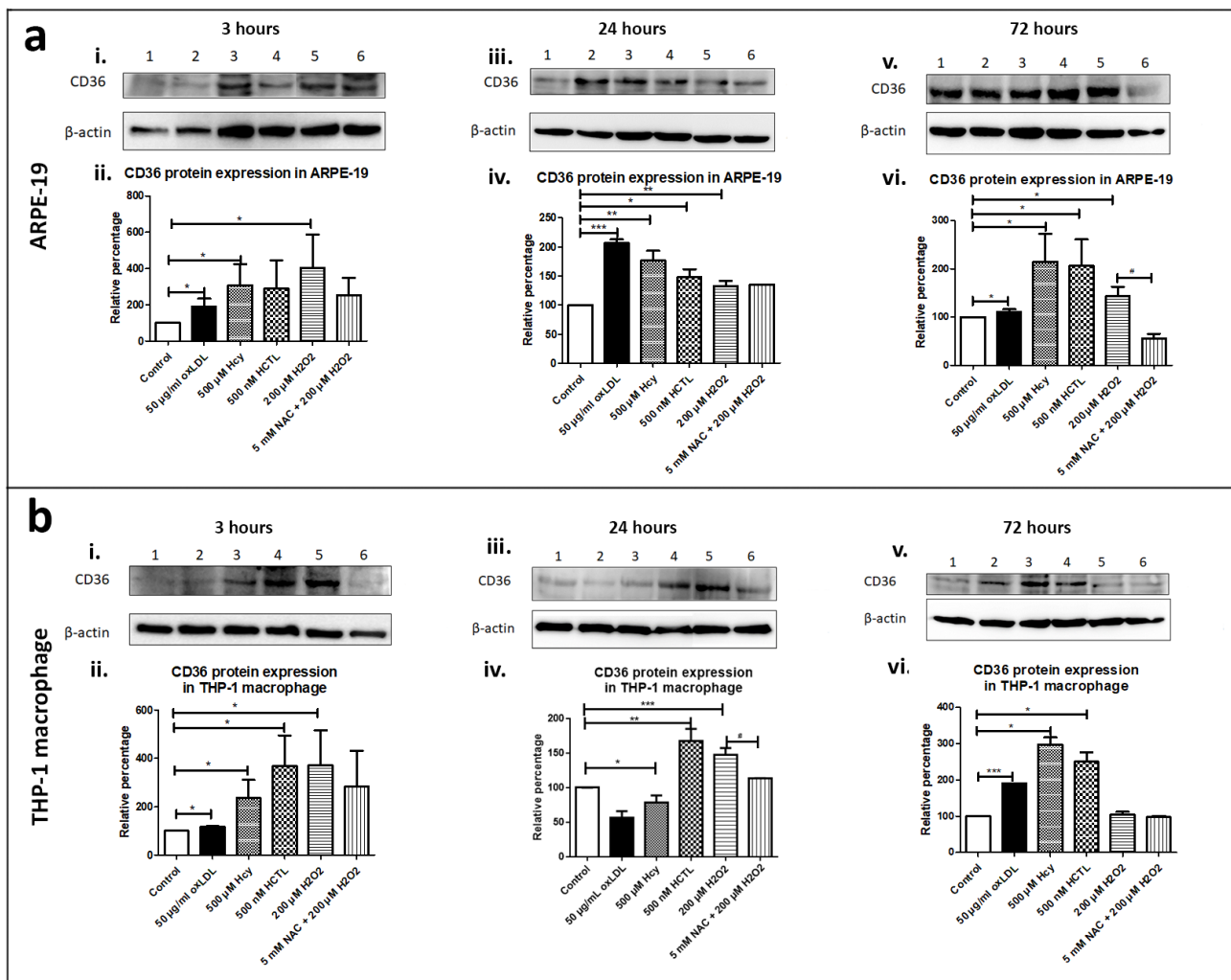


Figure 3

CD36 protein expression in ARPE-19 and THP-1 macrophage cells

Effect of the prooxidants on CD36 protein expression was analysed by Western Blot in (a) ARPE-19 and (b) THP-1 macrophage cells for (i, ii) 3 hours, (iii, iv) 24 hours and (v, vi) 72 hours exposure. The data is expressed as relative percentage with respect to control and normalized to endogenous control β-actin. The data represented from three independent experiments done not less than triplicate. *#*p* < 0.05, ***p* < 0.01, ****p* < 0.001, considered as significant.

*Control vs prooxidants, #H₂O₂ vs NAC + H₂O₂.

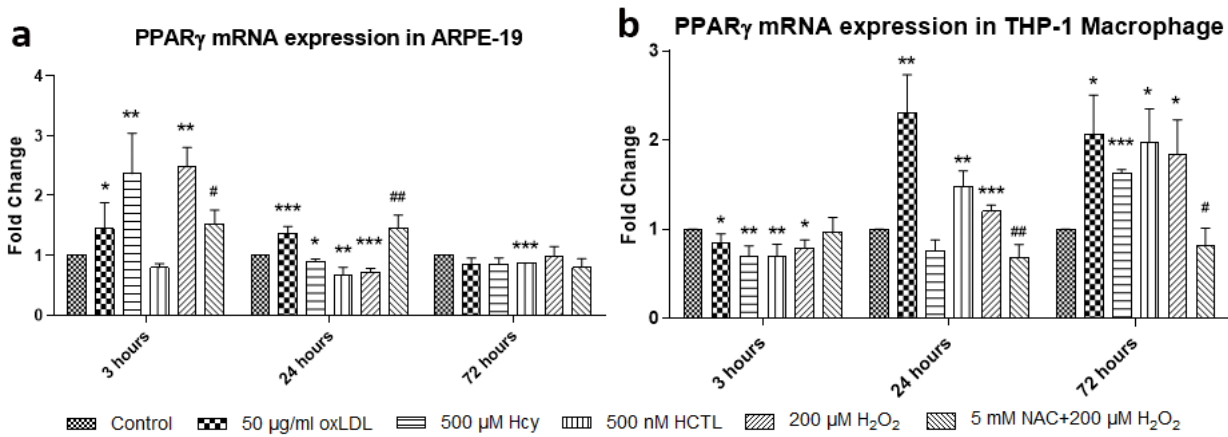


Figure 4

PPAR γ gene expressions in ARPE-19 and THP-1 macrophage cells

The bar graph showed the status of PPAR γ gene expressions under prooxidant conditions in (a) ARPE-19 and (b) THP-1 macrophage cells. The data represented from three independent experiments done not less than triplicate. *,# $p < 0.05$, **,## $p < 0.01$, *** $p < 0.001$, considered as significant. *Control vs prooxidants, #H₂O₂ vs NAC + H₂O₂.

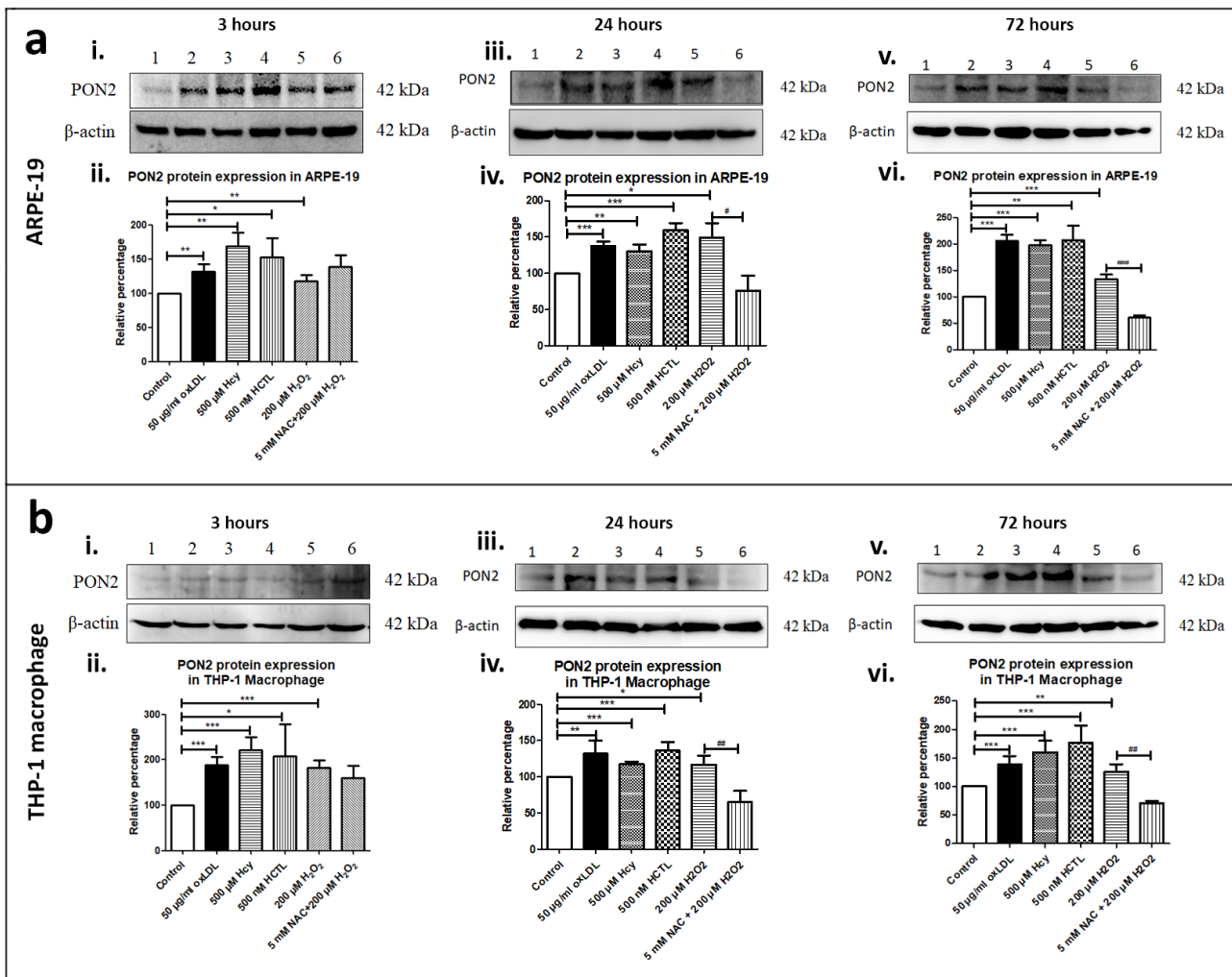


Figure 5

PON2 protein expression in ARPE-19 and THP-1 macrophage cells

Effect of prooxidants on PON2 protein expression was analysed by Western Blot in (a) ARPE-19 and (b) THP-1 macrophage cells for (i, ii) 3 hours, (iii, iv) 24 hours and (v, vi) 72 hours exposure. The data is expressed as relative percentage with respect to control and normalized to endogenous control β -actin. The

data represented from three independent experiments done not less than triplicate. $^{*}p < 0.05$, $^{**},\#\# p < 0.01$, $^{***},\#\#\# p < 0.001$, considered as significant. * Control vs prooxidants, $^{\#}H_2O_2$ vs NAC + H_2O_2 .

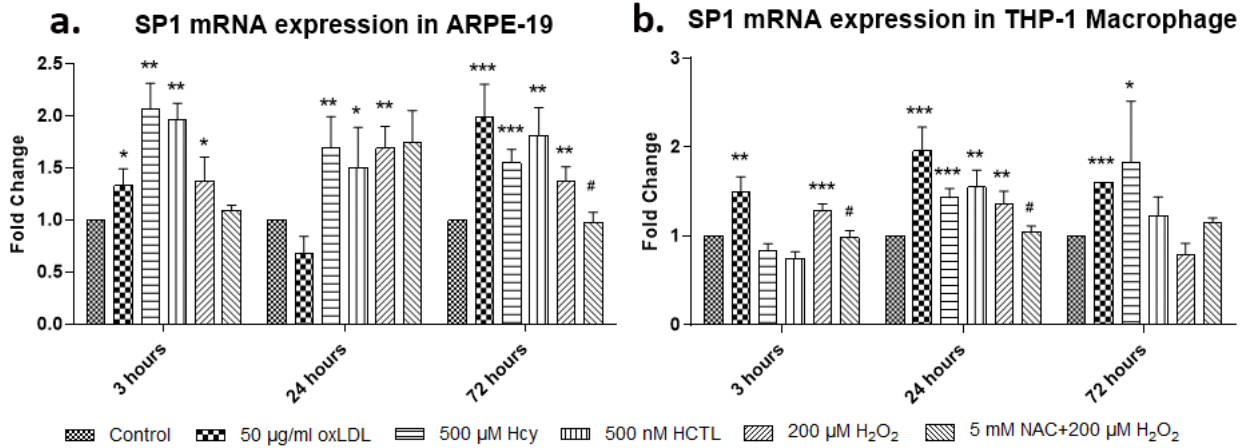


Figure 6

SP1 gene expressions in ARPE-19 and THP-1 macrophage cells

The bar graph showed the status of *SP1* gene expressions under prooxidant conditions in (a) ARPE-19 and (b) THP-1 macrophage cells. The data represented from three independent experiments done not less than triplicate. $^{*},\# p < 0.05$, $^{**} p < 0.01$, $^{***} p < 0.001$, considered as significant. * Control vs prooxidants, $^{\#}H_2O_2$ vs NAC + H_2O_2 .

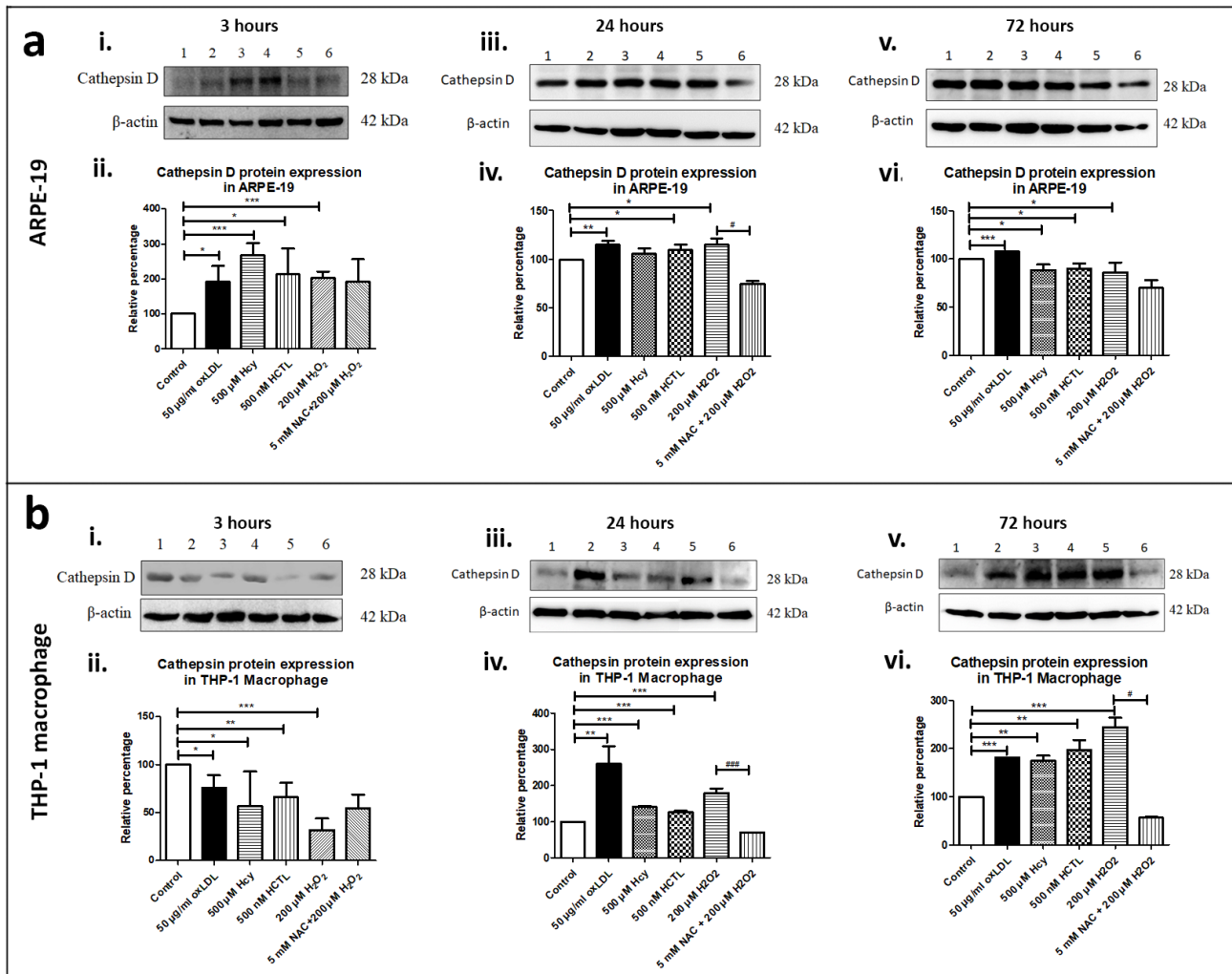


Figure 7

Cathepsin D protein expression in ARPE-19 and THP-1 macrophage cells

Effect of prooxidants on cathepsin D protein expression was analysed by Western Blot in (a) ARPE-19 and (b) THP-1 macrophage cells for (i, ii) 3 hours, (iii, iv) 24 hours and (v, vi) 72 hours exposure. The data is expressed as relative percentage with respect to control and normalized to endogenous control β -actin. The data represented from three independent experiments done not less than triplicate. $^*p < 0.05$, $^{**}p < 0.01$, $^{***},####p < 0.001$, considered as significant. * Control vs prooxidants, $^{\#}H_2O_2$ vs NAC + H_2O_2 .

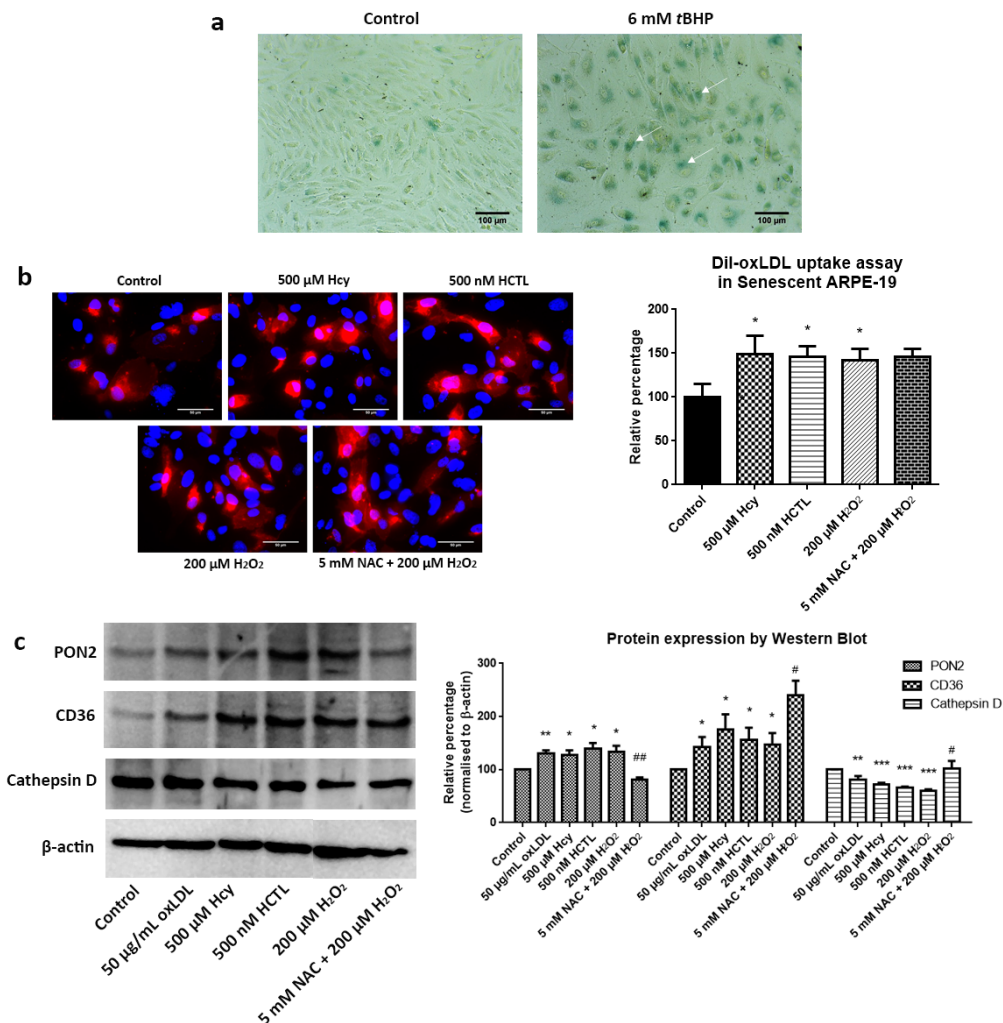


Figure 8

Effect of prooxidants on protein expressions and oxLDL uptake in senescent ARPE-19 cells

(a) Senescent-associated β -galactosidase activity (SA- β gal) of tert-Butyl hydroperoxide (tBHP) treated ARPE-19 cells. The senescence was confirmed by the blue coloured pigment formed in the tBHP treated ARPE-19 cells as shown by arrow. (b) DiI-oxLDL uptake was measured in sARPE-19 cells exposed to Hcy, HCTL, H_2O_2 and NAC + H_2O_2 conditions based on the pink immunofluorescence of the DiI. The bar graph showing the pixel intensity of the fluorescence analysed by Image J software. (c) Effect of prooxidants treatment on PON2, CD36 and Cathepsin D protein expression was analysed by western blot in sARPE-19 cells for 24h exposure. The values are expressed as Mean \pm SEM. The data represented from three independent experiments done not less than triplicate. $^*p < 0.05$, considered as significant. * Control vs prooxidants, $^{\#}H_2O_2$ vs NAC + H_2O_2 .

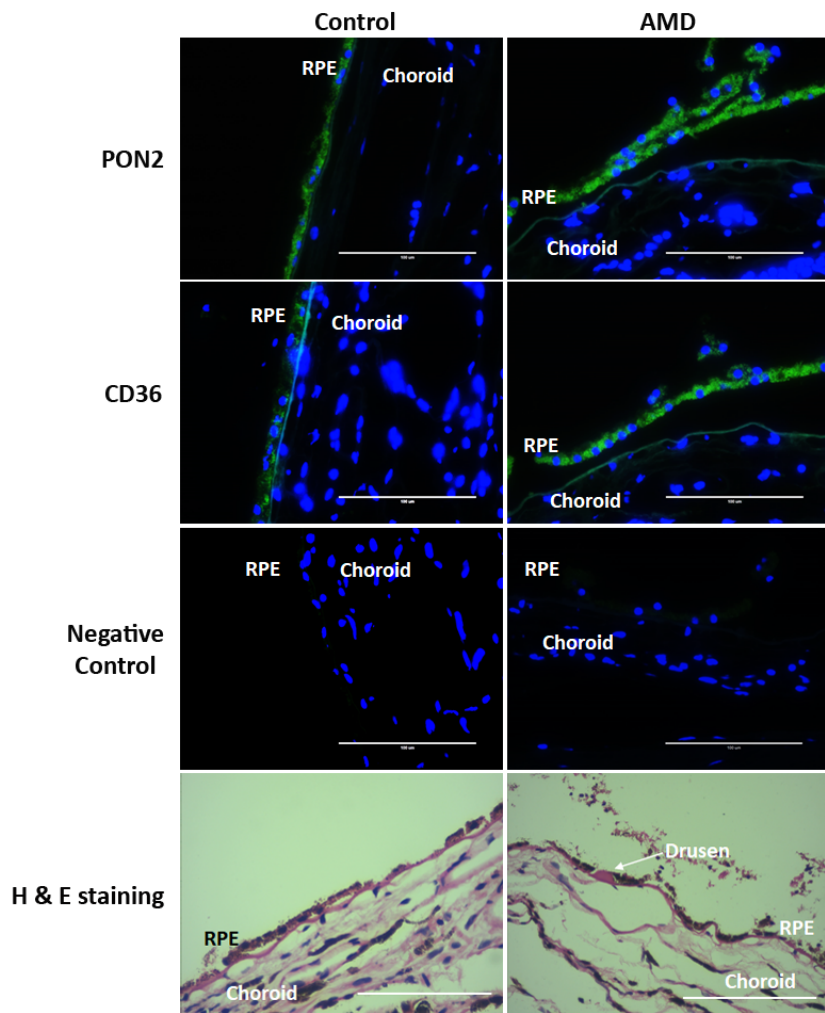


Figure 9

PON2 and CD36 expression in RPE of AMD and control eye tissues

Immunofluorescence for PON2 and CD36 (Green fluorescence) was observed in RPE of control and AMD eye tissue sections of paraffin blocks. Hoechst stain was used for nuclei staining (Blue fluorescence). The arrow mark in the Haematoxylin and Eosin (H & E) staining shows drusen in the AMD donor eye tissue. Image magnification: 40X; Scale bar: 100 μ m.

Supplementary Files

This is a list of supplementary files associated with this preprint. Click to download.

- [FigureS1.tif](#)
- [SupplementaryFile1.docx](#)